

INTRODUCTION

In high brightness electron accelerators, the beam dynamics and transport is strongly influenced by the space charge fields, which depend on the detail of the electronic distribution and its evolution along the beamline [1]. In linear beam dynamics, it is sufficient to monitor the second order moments of the distribution which has a constant shape along the beamline, but as soon as non-linear forces are applied, the distribution will evolve along the beamline. Having an accurate representation of the beam transverse phase space is then critical to predict the beam behavior in many setups.

Tomography is a well-developed imaging technique that uses a set of projections to reconstruct a distribution in a space with higher dimensions. Applied to beam physics, tomography can be used to reconstruct the 4D phase space distribution from an appropriately chosen set 2D transverse beam profile (projections) [2-5]. We present an algorithm to tomographically reconstruct the 4D phase space of a beam distribution of a high brightness electron beam, based on the use of two fluorescent screens separated by a beamline containing a quadrupole triplet which can be used to impart arbitrary rotation to the beam phase space. The reconstruction method is based on generating a macroparticle distribution which matches the initial profile and then it is iteratively updated using the beam projection on the second screen until convergence is achieved. This process is repeated for many quadrupole current settings. The algorithm is benchmarked against GPT simulations, and then implemented at the UCLA Pegasus beamline to measure the phase space distribution for an upcoming high speed electron microscope experiment [6-8].

METHODS

The reconstruction is performed on the setup currently installed at the UCLA Pegasus laboratory shown in Fig. 1. The initial spatial distribution is recorded on screen 4 and the various projections are obtained changing the currents in the green quadrupoles with the beam profile recorded on the final YAG screen. The current settings for the quadrupoles are chosen in order to maximize the range of angles the phase space rotates before hitting the final screen. The rotation angles used in both the simulation and the experiment are shown in Fig. 2.

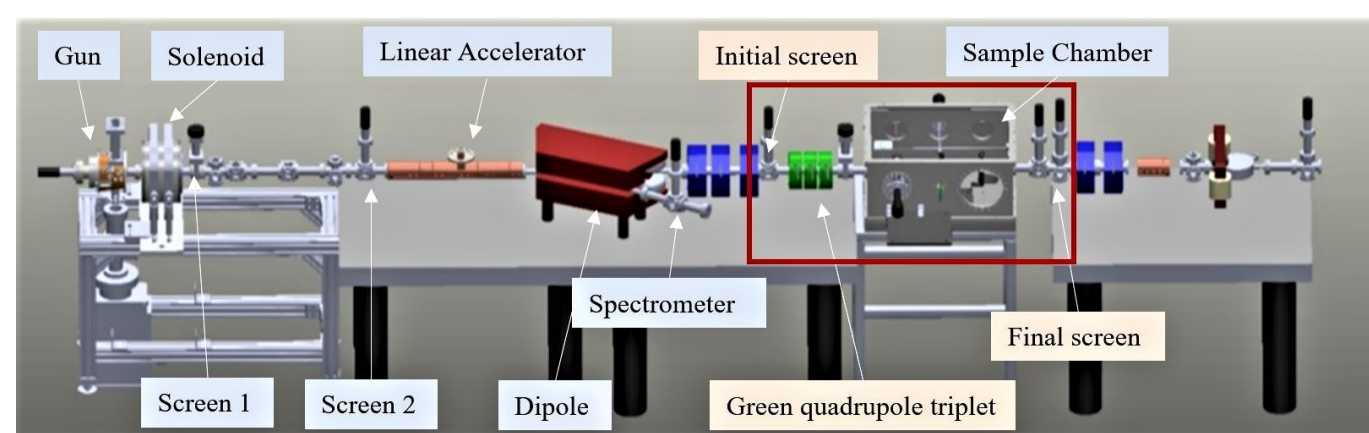


Figure 1: Schematic of the UCLA Pegasus beamline. The red box shows where the experiment takes place.

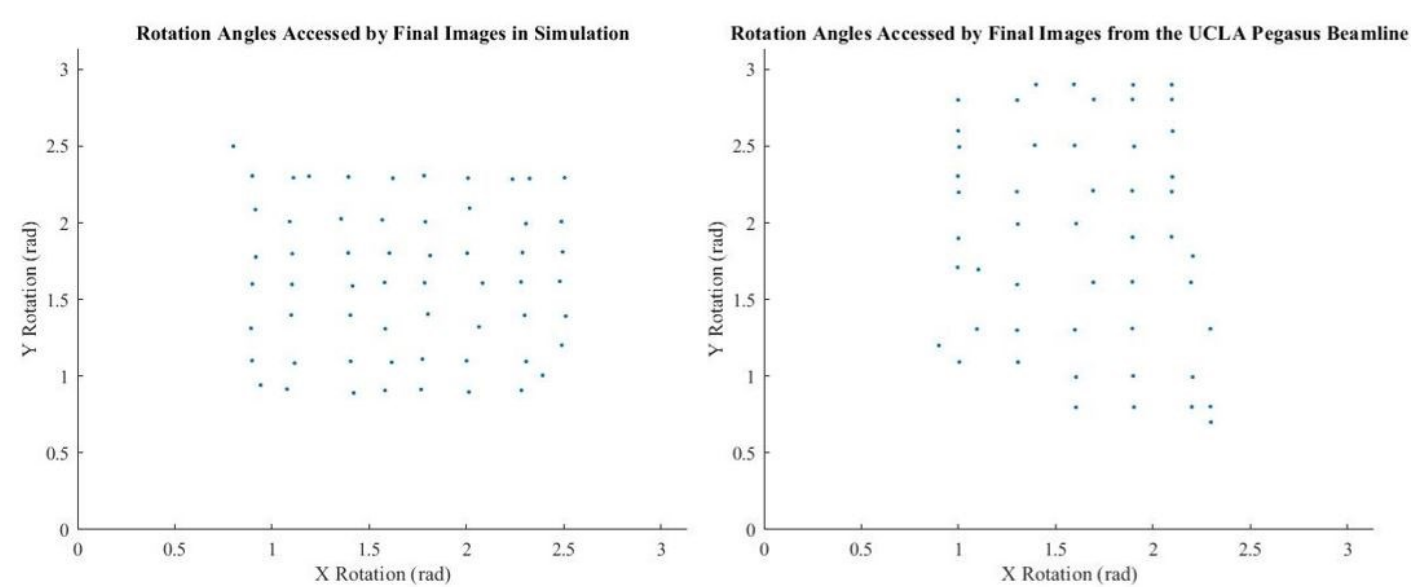


Figure 2: The rotation angles of each set of quadrupole settings used in simulation (left) and experiment (right).

land in the correct pixels for more than k images are respawned with values from a 4D normal distribution centered at 0 with standard deviation from the second-order moment matrix of the particles that survived the marking process. The algorithm terminates when the number of particles that need to be respawned is less than $p\%$ of the total number of macroparticles used.

To reconstruct the 4D transverse phase, we begin by initializing N macroparticles using the image at the initial screen as the probability distribution for the x - y coordinates. A random uniform momentum distribution is then assigned to the ensemble. For each set of quadrupole settings, the guess ensemble is transported to the final screen using the beam transport matrix. The final phase space is then projected onto the x - y plane and compared with the data image at the final screen. Particles that landed in pixels having excess charge compared to the measured image are marked to be respawned. After the marking process is repeated through all the quadrupole settings in the data sets, particles that failed to

RESULTS

Reconstruction of Simulation

To test the reconstruction algorithm, we generated a test data set using GPT formed by an initial screen image and 59 final screen images with different quadrupole current settings. The distribution to be reconstructed is shown in Fig. 3. Setting the convergence parameters to be $k = 1$ and $p = 1$, the algorithm was able to reconstruct the full 4D phase space in 7.46 s on a standard personal laptop using four cores. The reconstructed distribution is shown in Fig. 4.

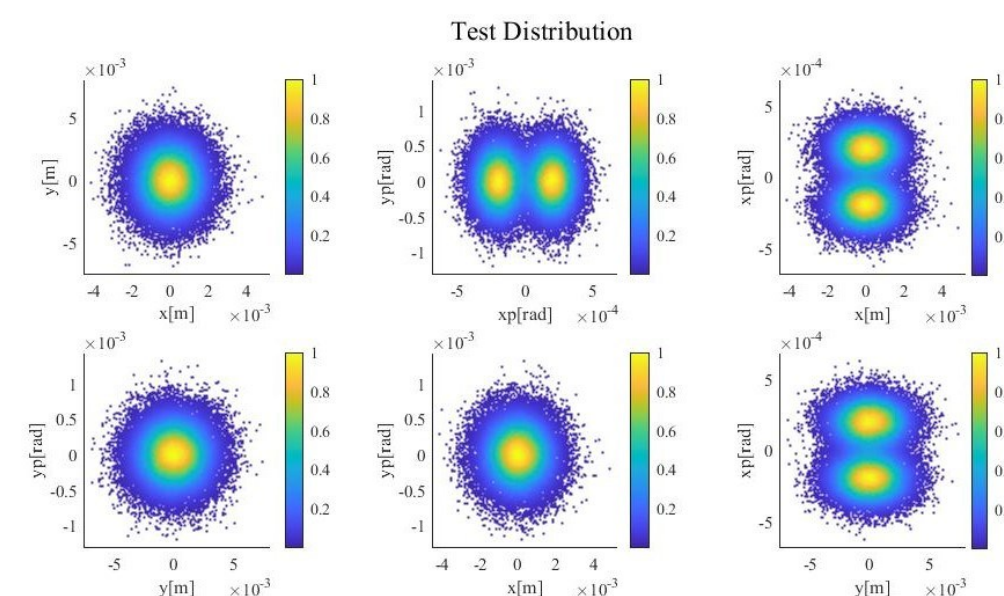


Figure 3: Simulated test distribution to be reconstructed.

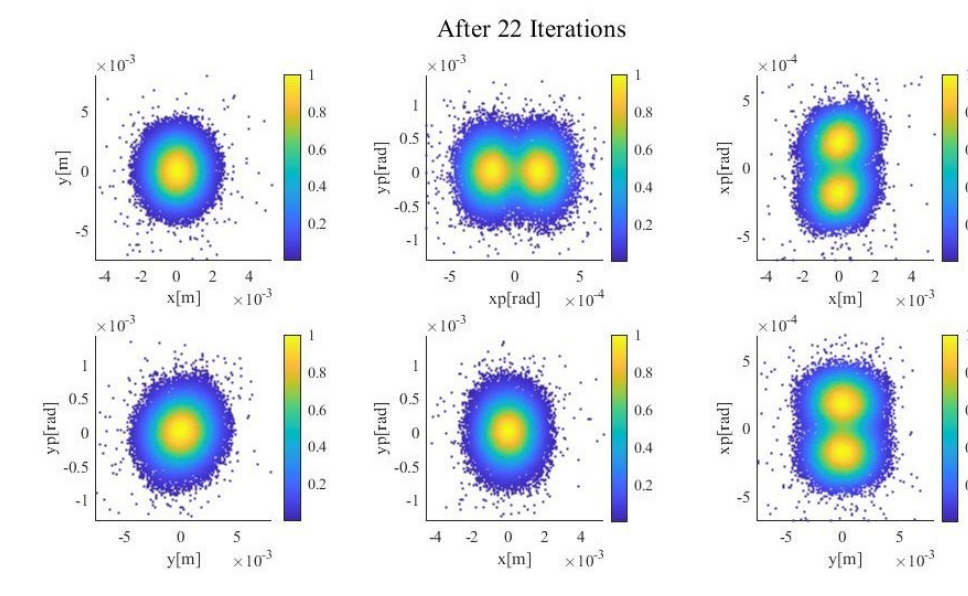


Figure 4: The reconstructed 4D phase space after 22 iterations of momentum reassignment.

Reconstruction of Experimental Data

The algorithm was used on experimental data collected from the UCLA Pegasus laboratory after the simulation successfully reconstructed the desired phase space. An initial screen image was taken at screen 4 and used as a probabilistic intensity mask to obtain the initial spatial distribution as shown in Fig. 5.

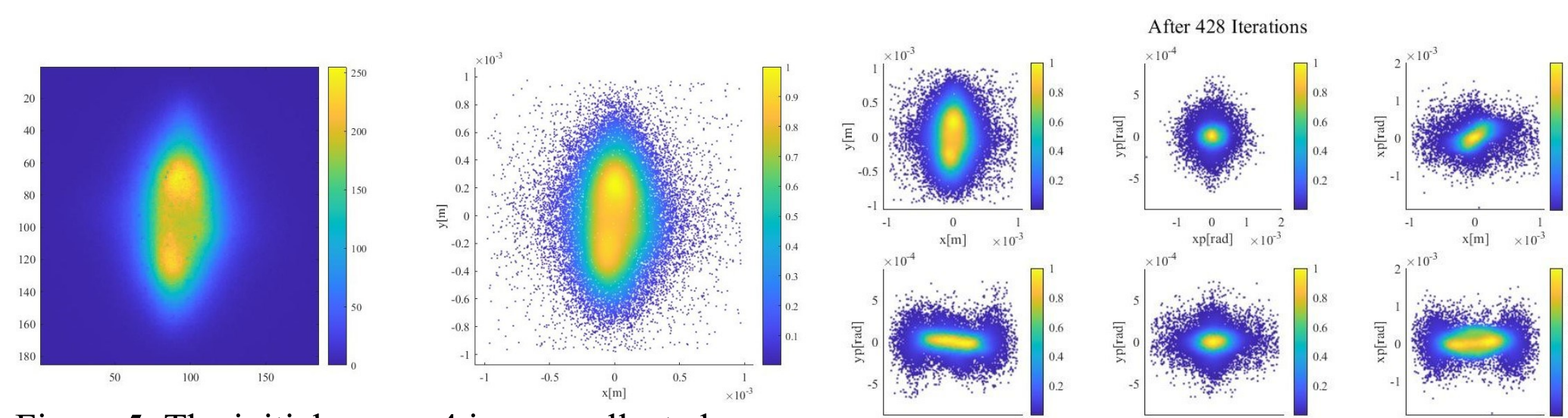


Figure 5: The initial screen 4 image collected from the UCLA Pegasus beamline (left) and the spatial distribution the algorithm initialized.

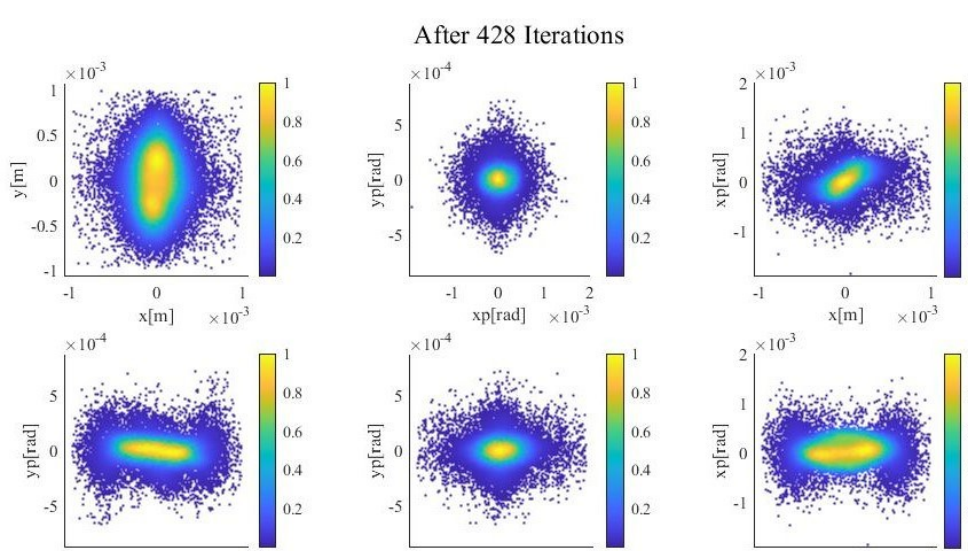


Figure 7: The reconstructed 4D phase space after 428 iterations of momentum reassignment.

At the final screen, 50 data images from the beamline were used for image comparison. Setting the algorithm's stopping parameter to be $k = 5$ and $p = 15$, the runtime is 361.78 s using four cores on a personal laptop. Figure 6 shows the comparison between the data images and the reconstructed phase space projections. The point-spread function used in the displayed trial is $18.63 \mu\text{m}$. The noise parameter from image filtering is set as 0.5 so that a particle will be marked to be respawned if $p_r - p_i > 0.5 \cdot \sqrt{p_i}$ where p_r is the pixel the particle lands in and p_i is the corresponding pixel from the target data image. The reconstructed distribution has a beam emittance of $1.6332 \times 10^{-15} [\text{m} \cdot \text{rad}]$. The distribution is shown in Fig. 7.

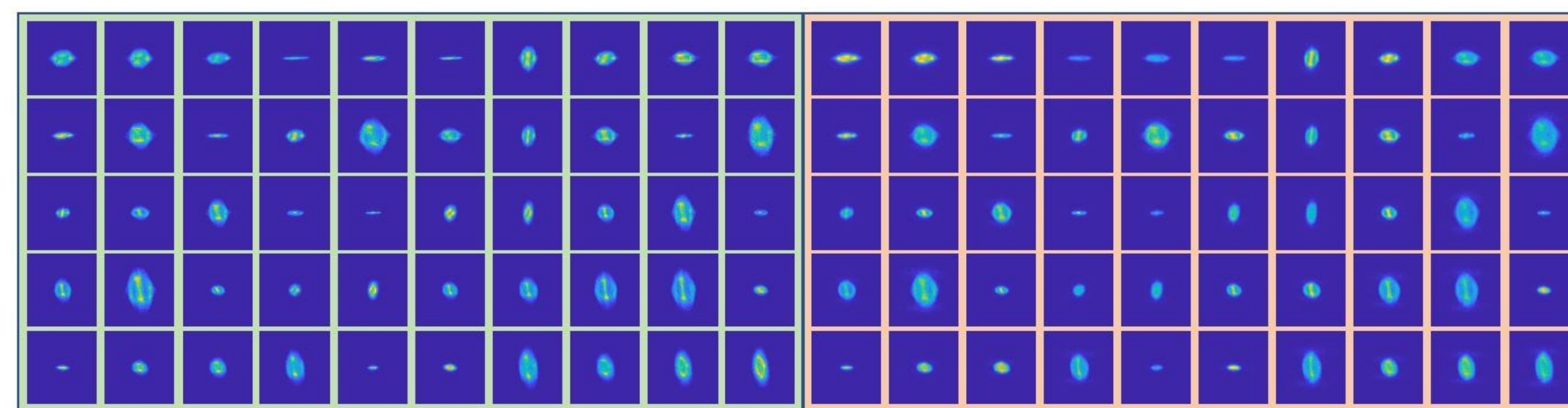


Figure 6: The left box contains 50 final images from the UCLA Pegasus beamline. The right box are the corresponding final images based on the reconstructed 4D phase space.

CONCLUSION

We have presented a method to tomographically reconstruct the full 4D transverse phase space distribution. The method uses one initial screen projection, three quadrupoles for beam rotation, and a final screen for spatial projections of the beam's final distribution. Using an iterative momentum reassignment algorithm, the method can reconstruct the full 4D phase space with reasonable computational time. We have verified the algorithm by applying it to a simulated distribution. Using images from GPT, the algorithm was able to reconstruct complicated inner patterns within the momentum space. The reconstructed distribution closely matches the original distribution.

The algorithm is then tested on data images collected from the UCLA Pegasus beamline. Although the reconstruction time is higher than in simulation, the algorithm can reconstruct a 4D transverse phase space that produces images that approximately matches the final spatial projections of the actual beam under 50 quadrupole-controlled rotations.

REFERENCES

- [1] P. Musumeci, J. G. Navarro, J. Rosenzweig, L. Cultrera, I. Bazarov, J. Maxson, S. Karkare, and H. Padmore, "Advances in bright electron sources," *Nuclear Instruments and Methods in Physics Research Section A: Accelerators, Spectrometers, Detectors and Associated Equipment*, vol. 907, pp. 209–220, 2018.
- [2] B. Hermann, V. A. Guzenko, O. R. Hürzeler, A. Kirchner, G. L. Orlandi, E. Prat, and R. Ischebeck, "Electron beam transverse phase space tomography using nanofabricated wire scanners with submicrometer resolution," *Physical Review Accelerators and Beams*, vol. 24, no. 2, p. 022802, 2021.
- [3] F. Hannon, I. Bazarov, B. Dunham, Y. Li, and X. Liu, "Phasespace tomography using the Cornell dc gun," in *11th biennial European Particle Accelerator Conference, EPAC*, vol. 8, 2008.
- [4] K. Hock, M. Ibsion, D. Holder, A. Wolski, and B. Muratori, "Beam tomography in transverse normalised phase space," *Nuclear Instruments and Methods in Physics Research Section A: Accelerators, Spectrometers, Detectors and Associated Equipment*, vol. 642, no. 1, pp. 36–44, 2011.
- [5] D. Xiang, Y.-C. Du, L.-X. Yan, R.-K. Li, W.-H. Huang, C.-X. Tang, and Y.-Z. Lin, "Transverse phase space tomography using a solenoid applied to a thermal emittance measurement," *Physical Review Special Topics-Accelerators and Beams*, vol. 12, no. 2, p. 022801, 2009.
- [6] D. Alesini, A. Battisti, M. Ferrario, L. Foggetta, V. Lollo, L. Ficcadenti, V. Pettinacci, S. Custodio, E. Pirez, P. Musumeci, et al., "New technology based on clamping for high gradient radio frequency photogun," *Physical Review Special Topics-Accelerators and Beams*, vol. 18, no. 9, p. 092001, 2015.
- [7] J. Maxson, D. Cesar, G. Calmasini, A. Ody, P. Musumeci, and D. Alesini, "Direct measurement of sub-10 fs relativistic electron beams with ultralow emittance," *Physical review letters*, vol. 118, no. 15, p. 154802, 2017.
- [8] P. Denham and P. Musumeci, "Space-charge aberrations in single-shot time-resolved transmission electron microscopy," *Physical Review Applied*, vol. 15, no. 2, p. 024050, 2021.

ACKNOWLEDGEMENT

This work has been supported by the National Science Foundation under Grant No. PHY-1549132 and grant PHY-1734215 and DOE grant No. DE-SC0009914. PD was supported by National Science Foundation under Grant No. DMR-1548924.